

Photon-counting 1.0 GHz-phase-modulation fluorometer

T. Mizuno, S. Nakao, Y. Mizutani, and T. Iwata

Citation: *Review of Scientific Instruments* **86**, 043110 (2015); doi: 10.1063/1.4917196

View online: <http://dx.doi.org/10.1063/1.4917196>

View Table of Contents: <http://scitation.aip.org/content/aip/journal/rsi/86/4?ver=pdfcov>

Published by the [AIP Publishing](#)

Articles you may be interested in

[Ultrashort dead time of photon-counting InGaAs avalanche photodiodes](#)

Appl. Phys. Lett. **94**, 231113 (2009); 10.1063/1.3151864

[Scalable time-correlated photon counting system with multiple independent input channels](#)

Rev. Sci. Instrum. **79**, 123113 (2008); 10.1063/1.3055912

[Direct determination of the free-carrier injection density, the free-carrier absorption, and the recombination factors in double heterostructure diodes by optical phase measurements. Part III](#)

J. Appl. Phys. **97**, 123536 (2005); 10.1063/1.1935741

[Measurements of picosecond lifetimes by time correlated single photon counting method: The effect of the refraction index of the solvent on the instrument response function](#)

Rev. Sci. Instrum. **75**, 3107 (2004); 10.1063/1.1790583

[Low cost phase-modulation measurements of nanosecond fluorescence lifetimes using a lock-in amplifier](#)

Rev. Sci. Instrum. **70**, 1535 (1999); 10.1063/1.1149620



Photon-counting 1.0 GHz-phase-modulation fluorometer

T. Mizuno, S. Nakao, Y. Mizutani, and T. Iwata^{a)}

Division of Energy System, Institute of Technology and Science, Tokushima University, 2-1 Minami-Jyosanjima, Tokushima 770-8506, Japan

(Received 12 September 2014; accepted 28 March 2015; published online 14 April 2015)

We have constructed an improved version of a photon-counting phase-modulation fluorometer (PC-PMF) with a maximum modulation frequency of 1.0 GHz, where a phase domain measurement is conducted with a time-correlated single-photon-counting electronics. While the basic concept of the PC-PMF has been reported previously by one of the authors, little attention has been paid to its significance, other than its weak fluorescence measurement capability. Recently, we have recognized the importance of the PC-PMF and its potential for fluorescence lifetime measurements. One important aspect of the PC-PMF is that it enables us to perform high-speed measurements that exceed the frequency bandwidths of the photomultiplier tubes that are commonly used as fluorescence detectors. We describe the advantages of the PC-PMF and demonstrate its usefulness based on fundamental performance tests. In our new version of the PC-PMF, we have used a laser diode (LD) as an excitation light source rather than the light-emitting diode that was used in the primary version. We have also designed a simple and stable LD driver to modulate the device. Additionally, we have obtained a sinusoidal histogram waveform that has multiple cycles within a time span to be measured, which is indispensable for precise phase measurements. With focus on the fluorescence intensity and the resolution time, we have compared the performance of the PC-PMF with that of a conventional PMF using the analogue light detection method. © 2015 AIP Publishing LLC. [<http://dx.doi.org/10.1063/1.4917196>]

I. INTRODUCTION

This paper reports in detail on the construction of an improved version of a photon-counting phase-modulation fluorometer (PC-PMF) and demonstrates the usefulness of this PC-PMF based on fundamental performance tests. The concept of the PC-PMF and the construction of the primary instrument to demonstrate the proof-of-principle have been reported previously by one of the authors.¹ However, at the time of publication, little attention was paid to the significance of the PC-PMF, apart from its capability for weak fluorescence measurements. Recently, we have fully recognized the importance of this instrument and its potential for fluorescence lifetime measurements, as described below.

Fluorescence lifetime measurements play important roles in a variety of fields, including analytical chemistry, biological chemistry, materials science, and medical applications. For example, in analytical chemistry, fluorescence lifetime values can be used to distinguish between two samples with similar spectral shapes that would otherwise be indistinguishable. When used in combination with a polarized-light measurement technique, fluorescence lifetime measurements allow us to obtain information on the dynamic behavior of specific molecules.²

Methods to obtain fluorescence lifetime values can be divided into two categories: time-domain (TD) methods and frequency-domain (FD) methods.^{3,4} In TD methods, the im-

pulse response of the fluorescent sample is measured, which allows us to obtain the fluorescence decay waveform directly. In contrast, FD methods correspond to techniques used to measure the steady-state response of the sample. Therefore, FD methods should be applied to biological samples that would be readily affected by the pulsed excitation light. In the early stages of FD instrument development, a PMF with a single modulation frequency was used. However, the PMF had two problems: (i) it was only applicable to fluorescent samples with impulse responses that were expressed as a single exponential function, i.e., it was not applicable to multicomponent samples and (ii) it was not applicable to low-quantum-yield fluorescent samples in principle. However, the first problem has been solved by adoption of plural modulation frequencies.^{5,6} One possible solution to the second problem is to use the PC-PMF that we have proposed here.

The initial PMF subsequently progressed to become the FD-PMF after the appearance of the high-repetition-frequency mode-locked laser (MLL).^{4,7} The output signal from a light detector such as a photomultiplier tube (PMT) was fed into a spectrum analyzer,^{3,8} or the signal waveform measured using a high-speed oscilloscope was Fourier-transformed. To derive the fluorescence lifetimes, the amplitude ratio and/or the phase differences between the reference signal and the fluorescence waveform at the fundamental modulation frequency and its harmonics were calculated. The FD-PMF enabled us to simultaneously determine lifetime values for multicomponent samples. Recently, a 10 GHz FD-PMF using a microchannel plate PMT (MCT-PMT) was reported, for which scrupulous attention was paid to the detection electronics.⁹ The MLL has also been used in TD instruments. In the TD method, the

^{a)}Author to whom correspondence should be addressed. Electronic mail: iwata@tokushima-u.ac.jp

use of the time-correlated single-photon-counting (TC-SPC) technique has become popular, where a combination of a time-to-amplitude converter (TAC) and a multichannel analyzer (MCA) operating in a pulse-height-analyzer (PHA) mode is used as a time analyzer. The resolution time per channel is less than 10 ps. At present, it is difficult to determine the drawbacks of these two types of MLL-based instrument. However, the two systems can be somewhat complicated and expensive. Additionally, the MLL system lacks the freedom to select the appropriate excitation wavelength for the sample under test.

However, the recent commercial availability of light-emitting diodes (LEDs) and laser diodes (LDs) in the blue and ultraviolet (UV) wavelength regions has changed the original concept slightly for fluorescence lifetime measurements;^{10–13} they have been adopted in the TD instruments and FD-PMFs. The use of LED or LD excitation light sources offers ease of construction and simple operation. Depending on the fluorescent sample, the LED (or LD) can be replaced with another device easily and quickly so that the emission wavelength matches the absorption wavelength of the target sample. This type of instrument is effective when we want to know the approximate fluorescence lifetime values for a specific purpose, such as screening of samples. In fact, a relatively inexpensive instrument with a LED or LD as a pulsed excitation light source is commercially available (for example, EasyLife™ series, Photon Technology International, Inc., NJ, USA).

The reason why the conventional PMF with a LD is reconsidered in this paper is that it offers an advantage over pulsed excitation instruments. Short fluorescence lifetimes can be obtained with high precision, even when using a relatively low modulation frequency. For example, a 10 ns-lifetime value can be obtained with precision, even when using a 5.0 MHz modulation frequency. In strict, in order to obtain the 10 ns-lifetime value with the highest sensitivity, the optimal modulation frequency should be 15.9 MHz, at which frequency the modulation ratio and the phase shift become $1/\sqrt{2}$ and $\pi/4$, respectively.^{2,21} However, even when the modulation frequency deviates from the optimal one, the phase measurement still works fairly well. This situation and reason can be explained qualitatively as follows: in the phase modulation method, we measure the steady-state response of the fluorescent system, whereas in the pulsed excitation method, we measure the impulse response of the system, as described above. Therefore, although we cannot make a simple and fair comparison, the phase modulation method has an advantage over the pulsed excitation method in terms of the amount of information per unit frequency, provided that the measurement time and the excitation power are identical. The use of a conventional PMF equipped with a LED (or LD) is therefore worthwhile. However, the conventional PMF was still difficult to use for measurement of multicomponent samples. To solve this problem, several promising techniques have been proposed, including variable frequency methods,^{14–16} Fourier transform-based methods,^{17,18} frequency-multiplexing methods,^{19,20} and a phase-modulated method.²¹

Although we have described that the PMF with LD is of use, it still has two technical problems that have not been

described clearly. The first problem concerns the light detector. A high-speed PMT is usually used as the fluorescence detector. The value of the load resistor for the PMT is thus commonly set to be 50 Ω to accommodate impedance matching to a 50 Ω -characteristic impedance coaxial cable and a 50 Ω -input impedance high-speed amplifier connected to the cable. In this setup, if we perform the analogue light detection procedure, then the average anode current of the PMT will easily exceed its absolute rating value. As a result, the cathode and the anode of the PMT are both easily damaged. If we use a larger load resistor value, the PMT cannot respond to the high modulation frequency. As a result, it is difficult to use a conventional PMT for “bright” fluorescent sample measurements; it is necessary to deliberately reduce the fluorescence intensity. However, a reduction in the fluorescence intensity results in a reduced signal-to-noise ratio (SNR). Although we can reduce the voltage applied to the PMT, this affects the response time of the PMT. The use of a Geiger-mode avalanche photodiode (APD) has been reported recently.^{22,23} However, it is hard to use this APD in many applications because the light detection area of such a high-speed APD is extremely small, e.g., 0.1×0.1 mm. The conventional PMF should therefore be applied to fluorescent samples with quantum efficiencies that are “moderately” high. The second problem with the conventional PMF is the attainable resolution time limitation. In general, the PMF’s high phase measurement precision capability was the reason why it was superior to the pulsed excitation method, as described above. However, the time constant of the resistor-capacitor (RC) low-pass filter formed at the output circuit of the PMT is approximately 2.5 ns for the $R = 50 \Omega$ load resistor and the stray capacitance of $C \cong 50$ pF. The stray capacitance consists of the output capacitance of the PMT itself and that of the coaxial cable connected to the PMT. Therefore, the fluorescence lifetime values of a few nanoseconds that were obtained lack reliability as a result, even if the mathematical deconvolution technique^{24,25} is introduced.

In a modern PMF, a heterodyne (or homodyne) technique is introduced to overcome such difficulties.^{26–33} Usually, the gain of the PMT is modulated at a frequency that is near (the same as) the modulation frequency of the excitation light source to generate a low beat frequency (dc) signal at the output of the PMT. Because the heterodyne (homodyne) detection technique reduces the frequency bandwidth of the system, the large value of the load resistor can be connected to the output of the PMT.^{20,29–31,33} In this fashion, the SNR and the sensitivity are improved, as was done by the conventional cross correlation technique.^{34–36} Resultantly, the precise phase (or amplitude) measurements for obtaining the fluorescence lifetime values are performed with success.²⁸ Nowadays, the heterodyne (homodyne) technique is introduced in the field of fluorescence lifetime imaging microscopy (FLIM), where a combination of a gain modulated image intensifier and a two-dimensional imaging camera is usually used.^{37–40} However, the heterodyne (homodyne) method still suffers from the limitation of the frequency bandwidth of the PMT or that of the image intensifier. As a result, the attainable resolution time in the fluorescence lifetime measurement is limited to a nanosecond order. Although the application of the heterodyne (homodyne) light detection method is preferable for use in the

low fluorescence intensity situation, it is still hard to use in the single photon situation, because the heterodyne (homodyne) method is inherently the analogue one.

Our proposed PC-PMF can solve above mentioned problems simultaneously: we have constructed a hybrid method, where a phase-domain measurement is conducted with TC-SPC detection electronics to circumvent the limitation of the response time and the low sensitivity. By introducing the TC-SPC technique into the conventional PMF, “extremely weak” fluorescence measurements can be realized. Because the aim of the PC-PMF is to perform weak light measurements, the problem of the damage to the anode (or cathode) electrode is alleviated at source. The resolution time attainable using the PC-PMF is exactly the same as that of the TC-SPC instrument, and high-speed measurements that exceed the frequency bandwidth of the PMT are possible. This is the outstanding advantage of the PC-PMF, in addition to its weak fluorescence measurement capability. While the problem of the total measurement time remains, it may be tolerated to an extent because the original aim was to measure weak fluorescence. Additionally, under extremely low fluorescence intensity conditions, it may be possible to enhance the measurement sensitivity by using a large load resistor value for the PMT and considering a trade-off between the sensitivity and the resolution time.^{20,29–31,33} Finally, we have to note that the role the PC-PMF and that of the heterodyne (or homodyne)-based PMF are different: the PC-PMF should be used when the high modulation frequency measurements, exceeding several hundreds of megahertz, and/or when the extremely low fluorescence intensity measurements are necessary, whereas the heterodyne-based PMF is used for the more general cases.

The PC-PMF that we reported previously was a primary version, in which an ultraviolet LED was used as the excitation light source with a maximum modulation frequency of 10 MHz. Therefore, the time span of the histogram waveform obtained from the MCA was less than one cycle of the modulation frequency for a given number of channels, and precise phase measurements were difficult. For precise phase measurements, it is essential to build a histogram waveform with multiple cycles in the time span and to increase the number of channels used. In our new version of the PC-PMF, we have used a LD as the excitation light source and have designed a stable LD driver with a modulation frequency of 1.0 GHz. We show that a histogram waveform with more than 50 cycles can be obtained for a time span of 50 ns when using 8192 channels. In this paper, we present the details of the high-performance PC-PMF. We also compare the proposed PMF with the conventional analogue version in terms of the applicable fluorescent intensity and the attainable resolution time.

II. PRINCIPLE OF OPERATION

Figure 1 shows a timing diagram to explain the principle of operation of the PC-PMF. Here, we note again that the PC-PMF is the combined instrument of the TC-SPC instrument (which is used in the pulsed excitation mode) and the conventional PMF (which is used in analogue light detection mode). Figure 1(a) shows a reference (or excitation) waveform that is sinusoidally modulated with a repetition frequency f (period

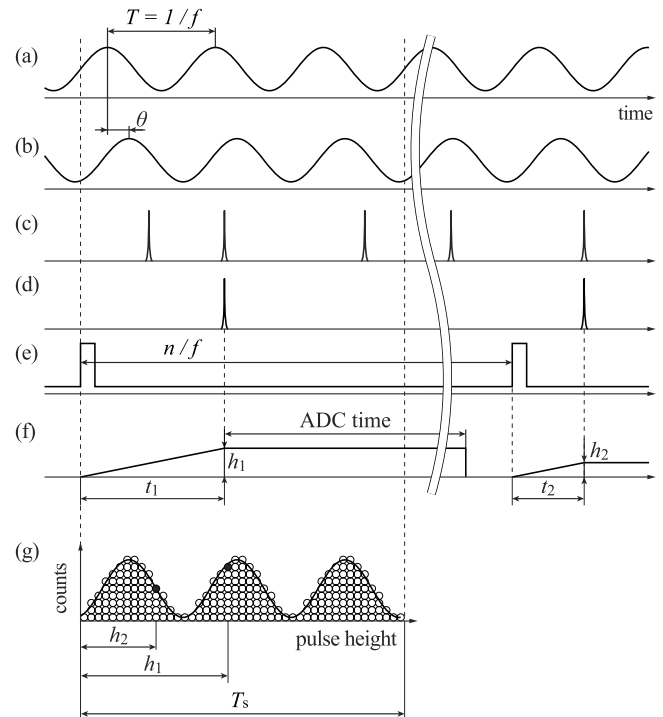


FIG. 1. Timing diagrams to explain the principles of operation of the PC-PMF: (a) a reference (or excitation) sinusoidal waveform with a modulation frequency $f = 1/T$, (b) a fluorescence waveform, (c) fluorescence photoelectron pulses when the fluorescence intensity is high, (d) a fluorescence photoelectron pulse when the fluorescence intensity is extremely low, (e) a trigger signal fed into the TAC, where the repetition frequency is f/n , (f) an output waveform obtained from the TAC, and (g) a histogram waveform that was statistically generated in the MCA.

$T = 1/f$). A typical fluorescence waveform of the type that would be obtained when the fluorescence intensity is high is shown in Fig. 1(b), where θ is the phase difference between the reference waveform and the fluorescence waveform. The conventional PMF using the analogue light detection method is used in this situation. The fluorescence lifetime value τ can be calculated from the following equation, $2\pi\tau f = \tan\theta$, using the measured value of θ and the known modulation frequency f , while assuming that the decay can be expressed by a single exponential function.

However, when the intensity of the fluorescence is low, we can no longer use the analogue light detection method. This is because the output signal obtained from the PMT becomes a multiple photoelectron-pulse situation, as shown in Fig. 1(c). The probability of the appearance of photoelectron pulses as a function of time is proportional to the magnitude of the analogue fluorescence waveform shown in Fig. 1(b). The lower fluorescence intensity limit to which we can apply the heterodyne-based (or homodyne-based) PMF is around in this situation. If the fluorescence intensity reaches an extremely low level, the output of the PMT becomes a single photoelectron scenario, as shown in Fig. 1(d); a maximum of one photoelectron pulse is generated for each excitation cycle. However, the probability of appearance of these photoelectron pulses is still the same as before. In this situation, we introduce the TAC, which is usually used in the TC-SPC technique in the TD method. The trigger signal that is fed into the start input terminal of the TAC is shown in Fig. 1(e); the frequency of the

signal is f/n , where n is the number of the frequency division for the modulation frequency f . The TAC measures the time intervals between the leading edge of the initial pulse and that of each photoelectron pulse, as shown in Fig. 1(f). The output signal from the TAC is fed into the MCA, which works in the PHA mode, where the TAC time span is T_s . The overall dead time of the “plus-one” procedure performed in the TAC and MCA pair to build the histogram is $8 \mu\text{s}$ in the present system, which is mainly because of the analogue-to-digital conversion (ADC) time. Therefore, the typical frequency of f/n becomes less than 125 kHz, as shown in Fig. 1(e). In a practical situation, however, we can increase the frequency f/n up to $1/T_s$, thanks to the next-arrival-pulse prohibition (disable) function of the TAC-MCA pair during the “plus-one” procedure, which enables the count efficiency to be enhanced (this topic will be discussed again in Sec. IV A). In this manner, after numerous excitation cycles, we can build a histogram waveform statistically as shown in Fig. 1(g), which shows the same waveform as that shown in Fig. 1(c) but with a time span of T_s .

By measuring the reference and fluorescence histogram waveforms sequentially, we can estimate the fluorescence lifetime value using the same data analysis procedure that was used for the conventional PMF. Introduction of the TC-SPC technique means that the nominal resolution time is improved in comparison with that of the conventional PMF.

III. INSTRUMENTAL SETUP

A. LD driver design

Figure 2 shows a LD driver circuit that was designed for the PC-PMF. The excitation light source used here was a violet LD (NDV4313; emission peak wavelength, 405 nm; maximum output power, 140 mW; threshold current, 35 mA; Nichia Co., Tokushima, Japan). The LD, however, can easily be replaced with another LD to match the excitation wavelength of the targeted sample to be measured.

The LD driver consists of two parts. The first part includes a transistor Q1 (BFG591; transition frequency, 7.0 GHz; maximum collector current, 200 mA; NXP Semiconductors, Eindhoven, Netherlands), which is used for the LD bias current control. The other part includes the same transistor (Q2) that was used for the high-frequency sinusoidal current modulation of the LD. By adopting these two transistors, the bias current

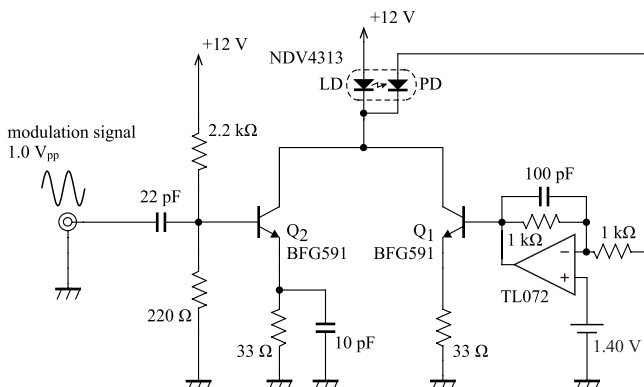


FIG. 2. Circuit diagram of the LD driver for high-frequency modulation.

and the modulation current can be controlled independently; the circuit design and the adjustment of the design are therefore simplified. This is the reason why one LD can be replaced with another so easily. The output power of the LD is monitored by a built-in photodiode (PD) and is used to stabilize the long-term working conditions via a negative feedback circuit. The cutoff frequency of this feedback circuit is approximately 100 kHz.

The degree of modulation of the LD at the modulation frequency of 100 MHz was approximately 75% when the bias current, the modulation current, and the average output power of the LD were 70 mA, 20 mA_{pp}, and 70 mW, respectively. Here, we defined the degree of modulation as the difference between the maximum and the minimum power divided by the averaged power. We have estimated this quantity from the reference waveform obtained from the PC-PMF system. Under the same conditions, the degree of modulation was 50% at the modulation frequency of 1.0 GHz. We thought that the modulation frequency of 1.0 GHz was the maximum frequency attainable by the entire PC-PMF system (this will be discussed in Sec. IV B).

B. Block diagram of the PC-PMF

Figure 3 shows a block diagram of the PC-PMF. The excitation light source and its driver were described in Sec. III A. The sinusoidal modulation signal for the driver is obtained from a phase-locked-loop (PLL) frequency synthesizer integrated circuit (ADF4350BCPZ; period jitter of <0.5 ps rms; Analog Devices, Norwood, MA, USA) with a reference oscillator (AWG520; period jitter of 6.0 ps rms; Tektronix, Beaverton, OR, USA). The reference oscillator typically generates a 10.0 MHz sinusoidal waveform and the PLL frequency synthesizer generates an up-converted frequency in the $f = 100 \text{ MHz} - 1.0 \text{ GHz}$ range. Fluorescence from the sample was fed into the PMT (R7400U, Hamamatsu Photonics K. K., Shizuoka, Japan) through a long-wavelength

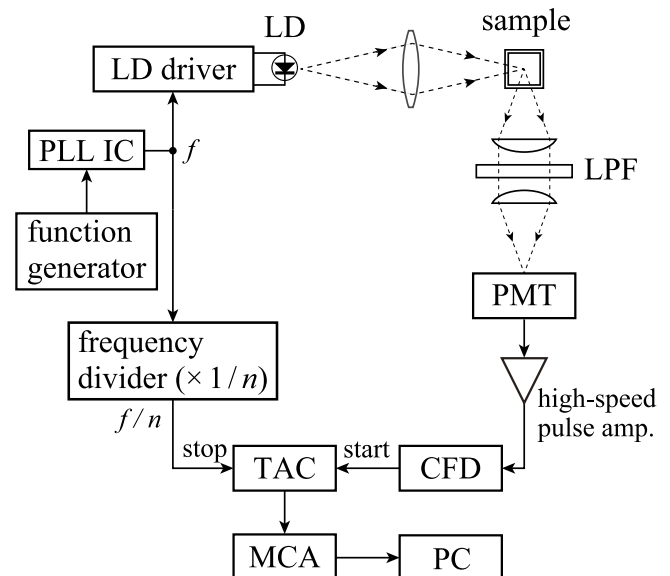


FIG. 3. Schematic block diagram of the PC-PMF. LD: laser diode, LPF: long-wavelength pass filter, PMT: photomultiplier tube, CFD: constant fraction discriminator, TAC: time-to-amplitude converter, MCA: multichannel analyzer, and PC: personal computer.

pass filter (LPF; SCF-50S-44Y, cutoff wavelength of 440 nm, Sigma Koki Co., Saitama, Japan). Where necessary, a neutral density filter (NDF) with an appropriate optical density value was inserted into the emission side to adjust the fluorescence intensity. The output photoelectron pulses obtained from the PMT were fed into a start-input terminal of the TAC (Type 566, Ortec, Oak Ridge, TN, USA) through a constant fraction discriminator (CFD; Type 584, Ortec, Oak Ridge, TN, USA). The stop pulse for the TAC was obtained from the function generator through a $1/n$ frequency divider. These connections for the start- and stop-input terminals of the TAC are the “reverse” connections that are frequently used to improve the count efficiency. The TAC output signal was finally fed into the MCA (TRUMP CARD 8k, Ortec, Oak Ridge, TN, USA) to build the histogram waveform.

When measuring the reference waveform, we replaced the fluorescent sample with a diffusion plate that has no wavelength dependency in reflection. The MCA has 8192 channels and the time span of the TAC is $T_s = 50$ ns. Therefore, the nominal resolution time given by the channel interval per single channel is 6.1 ps. In this setting, more than one cycle of the sinusoidal waveform can be recorded when $f > 20$ MHz. As described in Sec. III A, a major part of the total (or real) measurement time R in the present system is the ADC time ($8.0 \mu\text{s}$) of the TAC system. The maximum repetition frequency for construction of the histogram data is therefore limited to 125 kHz.

IV. MEASUREMENT RESULTS AND DISCUSSION

A. Linearity of the count efficiency and differential linearity

To demonstrate that the time analysis is performed in a normal manner by the TC-PMF, we have carried out two fundamental performance tests: the first checked the differential linearity of the channel interval and the second confirmed the linearity of the count efficiency Q for the uniformly distributed light. For these two purposes, we used the same procedure that was used for the conventional photon-counting time-analysis system.⁴¹

Because there is no actual definition of the count efficiency Q for the PC-PMF such as that proposed in the present paper, we have defined it here as $Q = Nn/Rf$, where N is the total number of counts in the histogram and R is the total (or real) measurement time; Q is the average number of photoelectron pulses counted during a single cycle of the frequency f/n . Because the value of Q varies depending on the time span T_s and the overall dead time ($\approx 8 \mu\text{s}$) of the “plus-one” procedure in the TAC-MCA pair, we fixed the frequency f/n to be 10 MHz; therefore, $Q = 10^{-7} \times N/R$. Because the definition of Q here is different to the definition used in the conventional TC-SPC system, in which Q is defined as the average number of photoelectron pulses per pulsed excitation, the value of Q in this paper has a relative meaning for the PC-PMF system only; we cannot make a direct comparison between the two systems.

Figure 4(a) shows a plot of Q versus incident light power P , where $R = 2400$ s. The light source used was a dc-driven

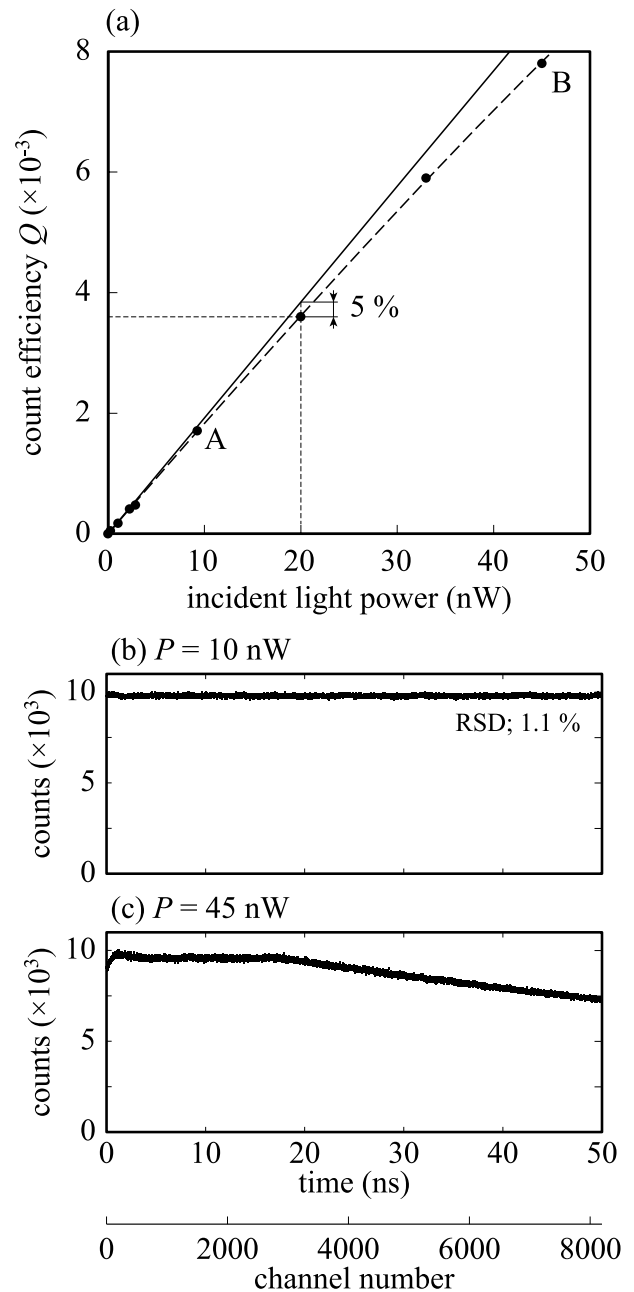


FIG. 4. (a) Plot of the count efficiency Q versus incident light power P for uniformly distributed incident light, (b) the differential linearity of the channel interval when $Q = 1.7 \times 10^{-3}$ ($P = 10$ nW) at point “A,” and (c) the same quantity when $Q = 7.8 \times 10^{-3}$ ($P = 45$ nW) at point “B.”

white LED (NSPW510BS, Nichia Co., Tokushima, Japan). The light power P incident on the PMT was varied in steps by inserting an appropriately valued ND filter and was calibrated using an optical power meter (Type 1830-c, Newport Co., Irvine, CA, USA). The linearity of Q as a function of P was maintained up to $Q = 4.0 \times 10^{-3}$, where we defined the upper limit of the linearity as a point that showed 5.0% deviation from the solid line shown in the plot. The light power corresponding to this 5.0% deviation point was 20 nW. We therefore concluded that the PC-PMF should be used when $P < 20$ nW to prevent waveform distortion.

Next, we evaluated the differential linearity (or the channel interval uniformity) for the same uniformly distributed

incident light. The experimental setup was the same as that used in the experiments above. Figure 4(b) shows a histogram waveform that was obtained under the conditions at a point “A” ($Q = 1.7 \times 10^{-3}$ and $R = 4790$ s for $P = 10$ nW), which lies in the linear range shown in Fig. 4(a). In this case, a flat-shaped histogram was obtained; the average count number per channel was 9945 and the relative standard deviation (RSD) was 1.1%. This result demonstrates the well-behaved differential linearity of the PC-PMF system; the statistics of the observed photoelectron pulses obeyed a Poisson distribution. For the case of point “B” ($Q = 7.8 \times 10^{-3}$ and $R = 940$ s for $P = 45$ nW), which lies in the nonlinear range in Fig. 4(a), the histogram waveform shown in Fig. 4(c) is slightly distorted by the count loss. Here, we have to note that a very small ripple is visible for time channels with a low index in Figs. 4(b) and 4(c). This distortion might be due to nonlinearity of TAC that we used.

B. Comparison of the PC-PMF with the conventional PMF

While the conventional PMF that uses the analogue light detection method is useful at moderately high fluorescence intensity levels, as mentioned in the Introduction, the proposed PC-PMF can be used in the extremely low intensity level range. To clarify the boundary level between the two systems, we have carried out comparative measurements using a reference waveform. The incident light power P on the PMT was varied in steps and was obtained directly from the sinusoidally modulated LD at $f = 100$ MHz.

The histogram waveforms shown in the left column of Fig. 5 are those obtained from the PC-PMF when (a) $P = 100$ nW, (b) $P = 10$ nW, and (c) $P = 1.0$ nW, where the maximum value in the histogram was fixed at 1.0×10^4 . The total measurement time R and the count efficiency Q in each case were (a) $R = 210$ s and $Q = 14.2 \times 10^{-3}$, (b) $R = 2370$ s and $Q = 1.7 \times 10^{-3}$, and (c) $R = 24120$ s and $Q = 0.17 \times 10^{-3}$, respectively. These three Q values lie on the linear range in Fig. 4(a). The dc background shown in each histogram is caused by the background that was originally presented in the LD emission and in the dark current of the PMT. Here, we note again that the data points in Figs. 5(b) and 5(c) for time channels at either edges were cropped to eliminate distortions due to the TAC nonlinearity.

In the right column of Fig. 5, we show the analogue waveforms that were recorded using a digital oscilloscope (TDS5054B; -3 dB cutoff frequency of 500 MHz; Tektronix, Beaverton, OR, USA), where (d) $P = 10 \mu\text{W}$, (e) $P = 1.0 \mu\text{W}$, and (f) $P = 100$ nW. We set the number of accumulations in the digital memory in the digital oscilloscope at 1.0×10^4 so that the waveforms appear clearly. The PMT used here was the same as that used in the PC-PMF, and the load resistance and the applied voltage were 50Ω and -900 V, respectively. When $P < 1.0 \mu\text{W}$, we cannot obtain the sinusoidal waveform at all via the conventional analogue light detection method because of the extremely low SNR. However, the sinusoidal histogram waveform was obtained correctly by the PC-PMF when $P < 10$ nW. When $P = 100$ nW, the histogram waveform was slightly distorted, because the PMT output was no longer in the single photoelectron condition. Even in this case,

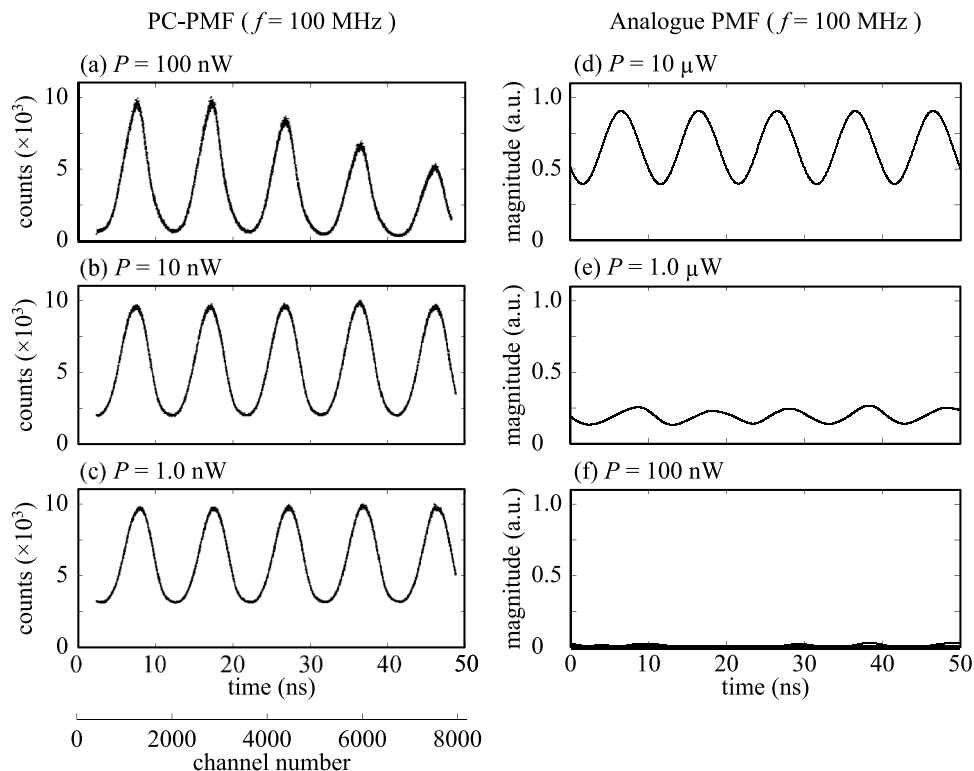


FIG. 5. Comparison of reference waveform ($f = 100$ MHz) obtained from the PC-PMF (left column) with that obtained from the conventional analogue light detection PMF (right column) for various incident light powers P on the PMT; (a) $P = 100$ nW, (b) $P = 10$ nW, (c) $P = 1.0$ nW, (d) $P = 10 \mu\text{W}$, (e) $P = 1.0 \mu\text{W}$, and (f) $P = 100$ nW. The analogue waveforms were accumulated by a digital oscilloscope with 1.0×10^4 times.

however, the PC-PMF can be used if we deliberately lower the light power that is incident on the PMT. The borderline at which the different methods should be used is approximately $P = 100$ nW.

C. Maximum modulation frequency and the resolution time

We have determined the maximum modulation frequency at which the PC-PMF works well. The maximum modulation frequency attainable using the present LD driver is 1.0 GHz, as described in Sec. III A. Figures 6(a)–6(c) show the histogram waveforms that were obtained from the PC-PMF for (a) $f = 250$ MHz, (b) $f = 750$ MHz, and (c) $f = 1.0$ GHz, respectively, where the maximum value in the histogram was fixed at 1.0×10^4 and a time span of only 20.0 ns is shown to clarify the plot. The incident light power on the PMT was $P = 10$ nW. The total measurement time and the count efficiency Q for the three cases were $R = 2400$ s and $Q = 1.7 \times 10^{-3}$, respectively. The values of Q are in the linear range shown in Fig. 4(a). The slight distortion on the envelope of the waveform in (c) might be because of the long term instability of the sinusoidal oscillator. For reference, we also show analogue waveforms measured by the digital oscilloscope in Figs. 6(d)–6(f), where $P = 10$ μ W, and we again set the number of accumulations at 1.0×10^4 . The -3 dB cutoff frequency of the oscilloscope was 500 MHz. The 1.0 GHz sinusoidal waveform was obtained successfully by the PC-PMF, but not by the analogue system. The frequency exceeds both the frequency bandwidth of the PMT and the

cutoff frequency of the oscilloscope. The frequency bandwidth of the PMT was determined by the time constant ($\cong 2.5$ ns) of the RC low-pass filter that was formed at the output of the PMT.

The capability to perform measurements that exceed the frequency bandwidth of the PMT is a significant advantage for the PC-PMF. The channel interval per single channel is 6.1 ps, which is determined based on the time span ($T_s = 50$ ns) of the TAC and the total number of channels (8192) of the MCA. However, the resolution time in detection is limited in practice by the time jitter induced by the PMT, which is mainly caused by the transit time spread of the photoelectron pulses running in the PMT (Type R7400U; applied voltage of -1000 V) and is approximately 0.3 ns.² While the best solution to reduce the time jitter is to use the MCT-PMT,⁹ we have reduced it to ≈ 0.17 ns by deliberately limiting the area of the PMT photocathode by using an appropriate aperture and by increasing the applied voltage up to -950 V. The overall resolution time of the PC-PMF system presented here is determined not only by the time jitter of the PMT but also by that of the LD emission. Empirically, we have estimated that the two jitters are roughly equal. The maximum modulation frequency for the LD described in Sec. III A was determined on this basis.

D. Fluorescence lifetime measurements by PC-PMF

To demonstrate the performance of the PC-PMF, we measured the fluorescence lifetime of 1.0 nM coumarin 152

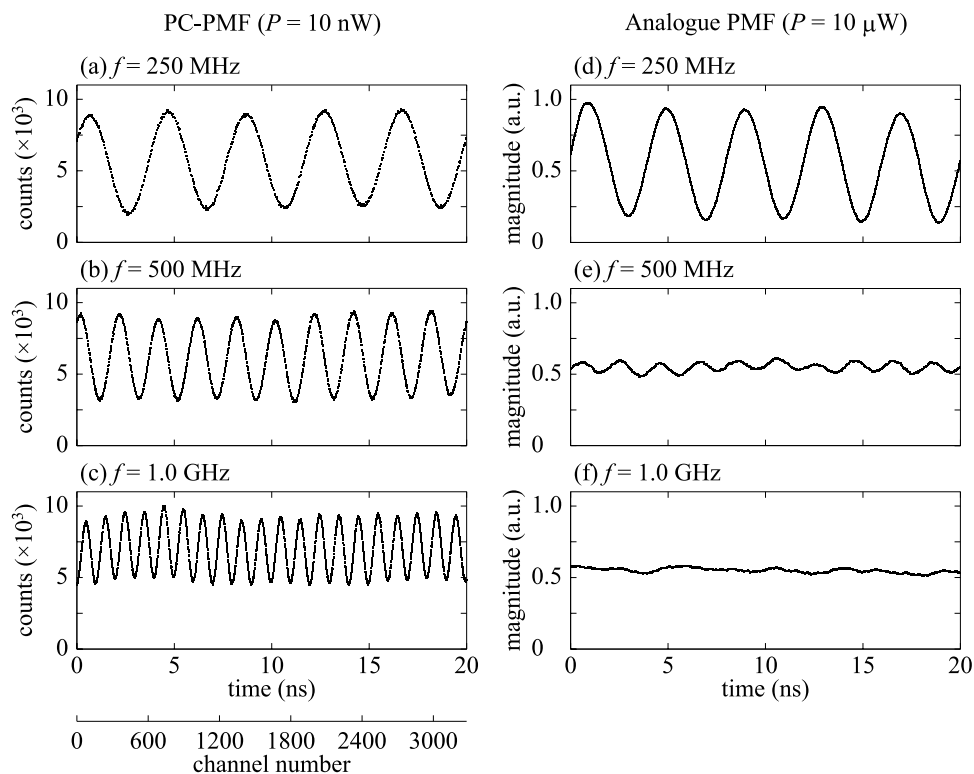


FIG. 6. Comparison of the reference waveforms obtained from the PC-PMF (left column) and the conventional analogue light detection PMF (right column) for various modulation frequencies; (a) $f = 250$ MHz, (b) $f = 500$ MHz, (c) $f = 1.0$ GHz, (d) $f = 250$ MHz, (e) $f = 500$ MHz, and (f) $f = 1.0$ GHz. The incident light power on the PMT was $P = 10$ nW for (a)–(c) and was $P = 10$ μ W for (d)–(f). The analogue waveforms were accumulated by a digital oscilloscope with 1.0×10^4 times.

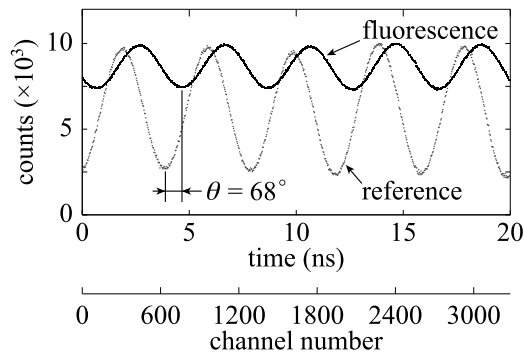


FIG. 7. Two histogram waveforms obtained from the PC-PMF: one is the reference waveform and the other is the fluorescence waveform obtained from 1.0 nM coumarin 152 in ethanol, where $f = 100$ MHz. The fluorescence lifetime estimated by assuming a single exponential component is $\tau = 1.6 \pm 0.1$ ns.

in ethanol, which is a standard fluorescent sample; the excitation wavelength and the emission wavelength were 405 and 480 nm, respectively. For the fluorescence measurement, we inserted the LPF (-3 dB cutoff wavelength of 440 nm; type SCF-50S-44Y, Siguma Koki Co., Saitama, Japan) on the emission side. However, the concentration of 1.0 nM is too low to be detected by the conventional analogue light detection method. Figure 7 shows two histogram waveforms; the first is the reference waveform and the other is the fluorescence waveform, and they were measured using the PC-PMF with $f = 100$ MHz, where $Q = 1.7 \times 10^{-3}$ and $R = 2400$ s. The fluorescence lifetime value was estimated using a convolved autoregressive model-based data analysis method³³ by assuming that a single component was $\tau = 1.6 \pm 0.1$ ns ($\theta = 68.0^\circ \pm 2.0^\circ$), which was in good agreement with the literature.⁴²

The next fluorescent sample that we measured was 1.0 mg/l DAPI (4',6-diamidino-2-phenylindole) in a Tris/EDTA (tris(hydroxymethyl)aminomethane/ethylenediaminetetraacetic acid) buffer solution, which is a fluorescent dye that is used for DNA probes. The excitation and emission wavelengths are 360 and 460 nm, respectively. We used the same 405 nm LD excitation light source as before at the cost of the excitation efficiency. We inserted the LPF (-3 dB cutoff wavelength of 440 nm; Type SCF-50S-44Y, Siguma Koki Co., Saitama, Japan) into the emission side. Figures 8(a)–8(c) show the histogram waveforms obtained from the PC-PMF for $f = 250$ MHz, 500 MHz, and 1.0 GHz, respectively, where (a) $\theta = 72^\circ$ for $Q = 1.7 \times 10^{-3}$ and $R = 2400$ s, (b) $\theta = 75^\circ$ for $Q = 1.7 \times 10^{-3}$ and $R = 2400$ s, and (c) $\theta = 80^\circ$ for $Q = 1.7 \times 10^{-3}$ and $R = 2400$ s. In each figure, the reference and fluorescence waveforms are shown. To ensure the clarity of the figure, a sinusoidal waveform with a time span of 20.0 ns is shown.

Figure 9 shows a plot of the phase difference versus the modulation frequency. The error bars attached to each plot were obtained from five measurements. If we assume that the decay is expressed by two exponential components, then the two estimated fluorescence lifetime values are $\tau_1 = 2.8 \pm 0.1$ ns and $\tau_2 = 0.19 \pm 0.05$ ns, with an initial amplitude ratio $a_2/a_1 = 2.7 \pm 0.1$. The solid line in Fig. 9 shows the estimated value. The two fluorescence lifetime values are in good agreement with those in the literature.⁴³

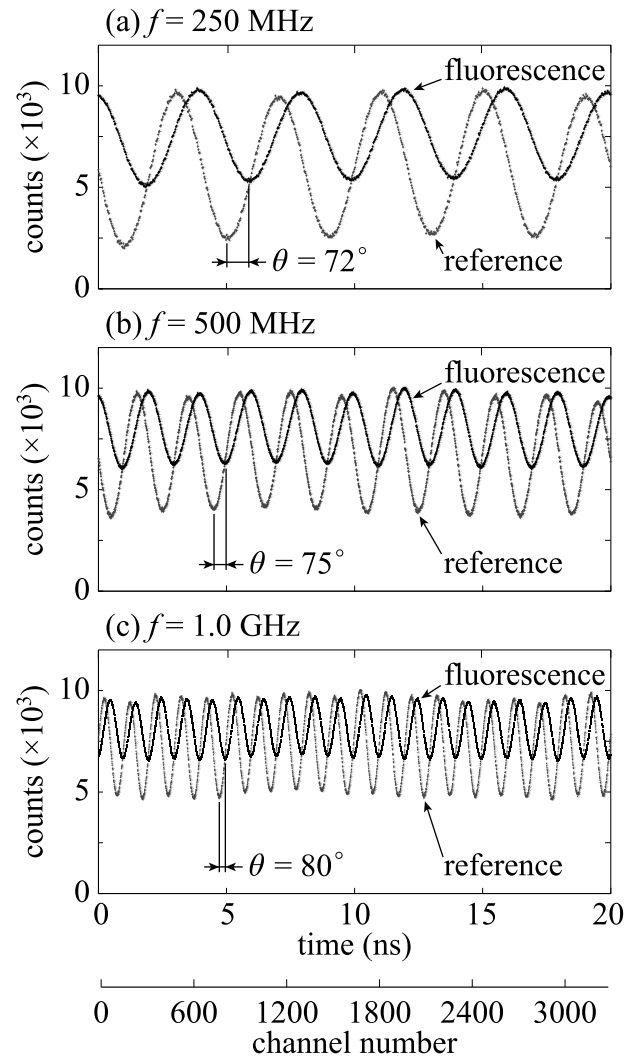


FIG. 8. (a) Two histogram waveforms obtained from the PC-PMF: one is the reference waveform and the other is the fluorescence waveform obtained from 1.0 mg/l DAPI in a Tris/EDTA solution, where $f = 250$ MHz, (b) the same as (a) but for $f = 500$ MHz, and (c) the same as (a) but for $f = 1.0$ GHz.

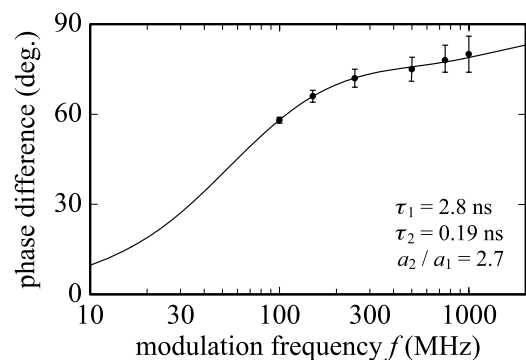


FIG. 9. A plot of the phase difference versus modulation frequency. The solid line shows the theoretically calculated value when assuming two components; $\tau_1 = 2.8 \pm 0.1$ ns and $\tau_2 = 0.19 \pm 0.05$ ns with an initial amplitude ratio $a_2/a_1 = 2.7 \pm 0.1$.

V. CONCLUSIONS

We constructed an improved version of the PC-PMF: a hybrid system was constructed where a phase domain measurement was conducted with TC-SPC detection electronics to

circumvent the limitation of the response time and the low sensitivity. The TC-PMF, which uses a LD as the excitation light source in combination with a laboratory-made driver is easy to construct and simple to operate. The maximum LD modulation frequency is 1.0 GHz, which exceeds the frequency bandwidth of the PMT. The introduction of the TC-SPC technique to the conventional PMF has proved effective, not only for measurements of low-quantum-yield fluorescent samples but also for enhancement of the resolution time. The proposed PC-PMF may be particularly useful for screening applications.

ACKNOWLEDGMENTS

This work was supported in part by a Grant-in-Aid for Scientific Research B (No. 26289066) from the Japan Society for the Promotion of Science (JSPS). We also thank an unknown reviewer for valuable comments and suggestions for improving the quality of this paper.

- ¹T. Iwata, A. Hori, and T. Kamada, "Photon-counting phase-modulation fluorometer," *Opt. Rev.* **8**, 326-330 (2001).
- ²J. R. Lakowicz, *Principles of Fluorescence Spectroscopy*, 3rd ed. (Springer, New York, 2006).
- ³F. V. Bright and G. M. Hieftje, "Rapid-scanning frequency-domain fluorometer with picosecond time resolution," *Appl. Opt.* **26**, 3526-3529 (1987).
- ⁴H. Merkelo, S. R. Hartman, T. Mar, and G. S. S. Govindjee, "Mode locked lasers: Measurements of very fast radiative decay in fluorescent systems," *Science* **164**, 301-302 (1969).
- ⁵G. Ide, Y. Engelborghs, and A. Persoons, "Fluorescence lifetime resolution with phase fluorometry," *Rev. Sci. Instrum.* **54**, 841-844 (1983).
- ⁶M. J. Wirth and S. H. Chou, "Phase-resolved subnanosecond spectroscopy using the beat frequencies from mode-locked lasers," *Appl. Spectrosc.* **42**, 483-486 (1988).
- ⁷R. D. Spencer and G. Weber, "Measurements of subnanosecond fluorescence lifetimes with a cross-correlation phase fluorometer," *Ann. N. Y. Acad. Sci.* **158**, 361-376 (1969).
- ⁸E. R. Menzel and Z. D. Popovic, "Picosecond-resolution fluorescence lifetime measuring system with a cw laser and a radio," *Rev. Sci. Instrum.* **49**, 39-44 (1978).
- ⁹G. Laczko, I. Gryczynski, Z. Gryczynski, W. Wicz, H. Malak, and J. R. Lakowicz, "A 10-GHz frequency-domain fluorometer," *Rev. Sci. Instrum.* **61**, 2331-2337 (1990).
- ¹⁰J. Sipior, G. M. Carter, J. R. Lakowicz, and G. Rao, "Blue light-emitting diode demonstrated as an ultraviolet excitation source for nanosecond phase-modulation fluorescence lifetime measurements," *Rev. Sci. Instrum.* **68**, 2666-2670 (1997).
- ¹¹T. Iwata, T. Kamada, and T. Araki, "Phase-modulation fluorometer using an ultraviolet light-emitting diode," *Opt. Rev.* **7**, 495-498 (2000).
- ¹²P. Herman and J. Vecer, "Frequency domain fluorometry with pulsed light emitting diodes," *Ann. N. Y. Acad. Sci.* **1130**, 56-61 (2008).
- ¹³P. Harms, J. Sipior, N. Ram, G. M. Carter, and G. Rao, "Low cost phase-modulation measurements of nanosecond fluorescence lifetimes using a lock-in amplifier," *Rev. Sci. Instrum.* **70**, 1535-1539 (1999).
- ¹⁴J. R. Lakowicz, G. Laczko, H. Cherek, E. Gratton, and M. Limkeman, "Analysis of fluorescence decay kinetics from variable-frequency phase shift and modulation data," *Biophys. J.* **46**, 463-477 (1984).
- ¹⁵E. Gratton, M. Limkeman, J. R. Lakowicz, B. P. Maliwal, H. Cherek, and G. Laczko, "Resolution of mixtures of fluorophores using variable-frequency phase and modulation data," *Biophys. J.* **46**, 479-486 (1984).
- ¹⁶J. R. Lakowicz and B. P. Maliwal, "Construction and performance of a variable-frequency phase-modulation fluorometer," *Biophys. Chem.* **21**, 61-78 (1985).
- ¹⁷T. Iwata, "Proposal for Fourier-transform phase-modulation fluorometer," *Opt. Rev.* **10**, 31-37 (2003).
- ¹⁸T. Iwata, H. Shibata, and T. Araki, "Construction of a Fourier-transform phase-modulation fluorometer," *Meas. Sci. Technol.* **16**, 2351-2356 (2005).
- ¹⁹T. Iwata, A. Muneshige, and T. Araki, "Analysis of data obtained from a frequency-multiplexed phase-modulation fluorometer using an autoregressive model," *Appl. Spectrosc.* **61**, 950-955 (2007).
- ²⁰T. Iwata, R. Ito, Y. Mizutani, and T. Araki, "Autoregressive-model-based fluorescence-lifetime measurements by phase-modulation fluorometry using a pulsed-excitation light source and a high-gain photomultiplier tube," *Appl. Spectrosc.* **63**, 1256-1261 (2009).
- ²¹T. Mizuno, Y. Mizutani, and T. Iwata, "Phase-modulation fluorometer using a phase-modulated excitation light source," *Opt. Rev.* **19**, 222-227 (2012).
- ²²T. Miyata, T. Iwata, and T. Araki, "A nanosecond-gate-mode-driven silicon-avalanche-photodiode and its application to measuring fluorescence lifetimes of Ce-doped YAG ceramics," *Meas. Sci. Technol.* **23**, 035501 (2012).
- ²³T. Miyata, T. Araki, and T. Iwata, "Correction of the intensity-dependent phase delay in a silicon avalanche photodiode by controlling its reverse bias voltage," *IEEE J. Quantum Electron.* **39**, 919-923 (2003).
- ²⁴T. Iwata, H. Shibata, and T. Araki, "Extrapolation of band-limited frequency data using an iterative Hilbert-transform method and its application for Fourier-transform phase-modulation fluorometry," *Meas. Sci. Technol.* **18**, 288-294 (2007).
- ²⁵T. Iwata, H. Shibata, and T. Araki, "A deconvolution procedure for determination of a fluorescence decay waveform applicable to a band-limited measurement system that has a time delay," *Meas. Sci. Technol.* **19**, 015601 (2008).
- ²⁶E. Gratton and M. Limkeman, "A continuously variable frequency cross-correlation phase fluorometer with picosecond resolution," *Biophys. J.* **44**, 315-324 (1983).
- ²⁷B. G. Pinsky and J. J. Ladasky, "Heterodyning of modulated pulses for fluorescence lifetime measurements in flow cytometry," *Proc. SPIE* **2137**, 794-799 (1994).
- ²⁸D. Kang and M. A. Kupinski, "Noise characteristics of heterodyne/homodyne frequency-domain measurements," *J. Biomed. Opt.* **17**, 015002 (2012).
- ²⁹T. Iwata, T. Takasu, and T. Araki, "Simple photomultiplier-tube internal-gating method for use in subnanosecond time-resolved spectroscopy," *Appl. Spectrosc.* **57**, 1145-1150 (2003).
- ³⁰T. Iwata, T. Inoue, and T. Araki, "Pseudo lock-in light detection method for a gain-modulated photomultiplier-tube," *Opt. Rev.* **11**, 19-23 (2004).
- ³¹T. Iwata, H. Ochi, and T. Araki, "A proposal of a pseudo-lock-in light-detection scheme by sinusoidal modulation of bias voltages applied to two dynodes in a photomultiplier tube," *Meas. Sci. Technol.* **20**, 065901 (2009).
- ³²B. Yuan, S. R. McClellan, B. F. Al-Mifgai, E. A. Growney, and O. A. Komolafe, "A cost-efficient frequency domain fluorescence lifetime measurement system," *Am. J. Phys.* **78**, 28-34 (2010).
- ³³T. Iwata, H. Kiyoto, Y. Mizutani, and T. Araki, "Comparison of a pulsed-excitation and a phase-modulation method for estimating fluorescence lifetimes using a convolved-autoregressive model and a high-gain PMT," *Opt. Rev.* **17**, 513-518 (2010).
- ³⁴J. M. Ramsey, G. M. Hieftje, and G. R. Haugen, "Time-resolved fluorimetry via a new cross-correlation method," *Appl. Opt.* **18**, 1913-1920 (1979).
- ³⁵R. E. Russo and G. M. Hieftje, "Determination of atomic and molecular excited-state lifetimes using an optoelectronic cross-correlation method," *Appl. Spectrosc.* **36**, 92-99 (1982).
- ³⁶D. L. Burden, S. E. Hobbs, and G. M. Hieftje, "Fluorescence lifetime measurement via a radionuclide-scintillation light source and analog cross correlation," *Anal. Chem.* **69**, 1936-1941 (1997).
- ³⁷X. F. Wang, T. Uchida, and S. Minami, "A fluorescence lifetime distribution measurement system based on phase-resolved detection using an image dissector tube," *Appl. Spectrosc.* **43**, 840-845 (1989).
- ³⁸J. R. Lakowicz and K. W. Berndt, "Lifetime-selective fluorescence imaging using an rf phase-sensitive camera," *Rev. Sci. Instrum.* **62**, 1727-1734 (1991).
- ³⁹X. F. Wang, T. Uchida, D. M. Coleman, and S. Minami, "A two-dimensional fluorescence lifetime imaging system using a gated image intensifier," *Appl. Spectrosc.* **45**, 360-366 (1991).
- ⁴⁰T. W. J. Gadella, Jr., T. M. Jovin, and R. M. Clegg, "Fluorescence lifetime imaging microscopy (FLIM): Spatial resolution of microstructures on the nanosecond time scale," *Biophys. Chem.* **48**, 221-239 (1993).
- ⁴¹T. Iwata, T. Uchida, and S. Minami, "A nanosecond photon-counting fluorimetric system using a modified multichannel vernier chronotron," *Appl. Spectrosc.* **39**, 101-109 (1985).
- ⁴²S. Nad, M. Kumbhakar, and H. Pal, "Photophysical properties of coumarin-152 and coumarin-481 dyes: Unusual behavior in nonpolar and in higher polarity solvents," *J. Phys. Chem. A* **107**, 4808-4816 (2003).
- ⁴³M. L. Barcellona and E. Gratton, "The fluorescence properties of a DNA probe," *Eur. Biophys. J.* **17**, 315-323 (1990).